Dynamic Mode Decomposition of Hydrofoil Cavitation

Jiahao Jia, Juanjuan Qiao and Tingrui Liu*
College of Mechanical & Electronic Engineering, Shandong University of Science & Technology, Qingdao 266590, China

Keywords: Dynamic Mode Decomposition, DMD.

Abstract: This study performs dynamic mode decomposition (DMD) for the NACA66 cavitation process, and the obtained modes have stable linear characteristics. The diagrams of different modes and the frequency energies of the corresponding modes are also analyzed. We found that these different modes capture the flow characteristics at different frequencies. The mean mode (Mode1) represents the basic flow structure and plays a dominant role in the cavitation process. Mode2 denotes the cavitated region, and Mode3 and Mode4 represent the cavitated stretch off. The higher-order modes represent the alternating shedding of cavitation and some high-frequency characteristics in the cavitation. The research in this study is essential for our understanding of the three-dimensional characteristics of the flow field during cavitation and the three-dimensional dynamical mode characteristics.

1 INTRODUCTION

During the operation of hydraulic machinery, when the partial pressure is less than the saturated vapor pressure of water, the form of water will change from liquid to vapor, called cavitation. With the decrease of the cavitation number, the cavitation phenomena are successively manifested as cavitation inception, sheet cavitation, cloud cavitation, and supercavitation. Cavitation has obvious unsteady characteristics, and it is easy to cause adverse effects on the hydrofoil, such as pressure fluctuation, vibration, noise, and erosion (Asnaghi, 2018; Dang, 2019). Hydrofoils are the most fragile and most prone to unsteady cavitation among turbomachinery, propeller, and other devices. Therefore, it is crucial to analyze hydrofoil cavitation and understand the physical mechanisms involved in this destabilizing phenomenon.

Scholars and experts in related fields have done a lot of research work to analyze the physical principles of cavitation and use various methods to predict and analyze the cavitation phenomenon. It contains two data-driven methods for research, POD (proper orthogonal decomposition) and DMD (dynamic mode decomposition) (Taira, 2020; Taira, 2017). Both ways use previous experimental or simulated data to analyze and predict the development of cavitation.

Liu (Liu, 2019) used POD and DMD methods for the coherent structure of ALE15 hydrofoil cavitation. They found that DMD is more advantageous than POD for decomposing complex flows into uncoupled coherent structures. Chen (Chen, 2012) proposed an improved DMD method and tested it in low Reynolds number in-cylinder fluid flow. To achieve a balance between the number of modes and computational efficiency, Jovanović (Jovanović, 2014) proposed sparsity to facilitate Sparsity-promoting dynamic mode decomposition DMD, which performed well in Poiseuille flow, supersonic flow, and two-cylinder jet. Kou and Zhang (Kou, 2017) proposed an additional criterion DMD (DMDc), which uses an improved criterion to align the flow modes and performs well in airfoil flutter. Grilli (Grilli, 2012) used the DMD method to study the unstable behavior of the shock-turbulent boundary layer and obtained that the low-frequency mode was related to the separation and impact of the bubble.

Although predecessors have conducted extensive and in-depth research on cavitation, it can be seen that dynamic mode decomposition is a relatively new analysis and research method by combing the latest recent research, so it has high research value. In this study, the unsteady cavitation process of NACA66 was analyzed by DMD. The contour of different modes are shown, and the frequency energy of different modes is analyzed. We found that these modes capture the flow characteristics at different frequencies. The research in this study is of great significance for us to understand the three-dimensional characteristics of the flow field and the three-dimensional dynamic mode characteristics in the cavitation process.

Jia, J., Liu, T. and Qiao, J.
Dynamic Mode Decomposition of Hydrofoil Cavitation.
DOI: 10.5220/0012150100003562
In *Proceedings of the 1st International Conference on Data Processing, Control and Simulation (ICDPCS 2023)*, pages 102-108
ISBN: 978-989-758-675-0

2 NUMERICAL SIMULATION AND METHODOLOGY

2.1 Numerical Simulation

The numerical simulation of the NACA66 hydrofoil is carried out, and the computational domain is a square tunnel with a length of 1000mm and a width of 192mm, as shown in Figure 1. The leading edge of the hydrofoil is 2c away from the velocity inlet, and the angle of attack(AOA) is 6°. The turbulence model adopts SST k-omega, and the cavitation model chooses Schnerr-Sauer. Then the inlet boundary condition is set to velocity inlet, and the velocity is set to 5.33m/s. The outlet boundary condition is set to the pressure outlet, and the pressure is set to 19000Pa. Finally, the no-slip boundary conditions are set on both side walls, and the upper and lower walls are set with slip walls.

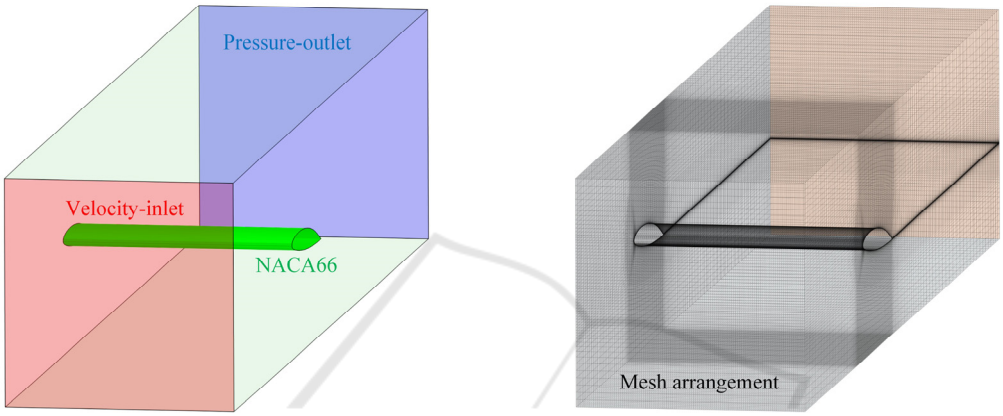

Figure 1: Computing domain and mesh arrangement.

2.2 Methodology

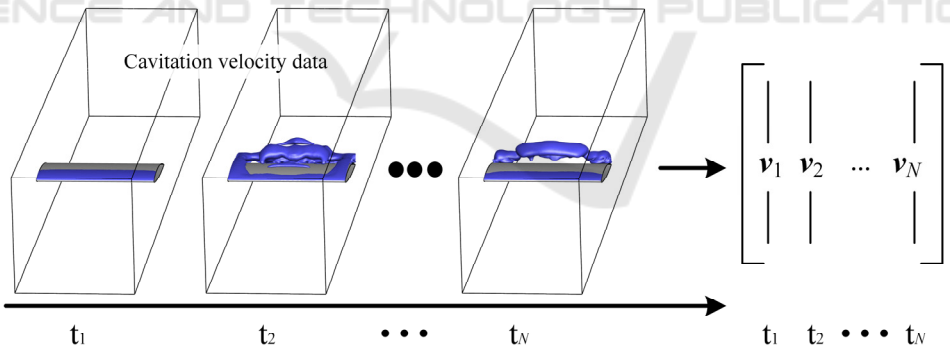

Figure 2: Matrix of cavitation velocity data.

This chapter introduces the basic principles and steps of the Dynamic Mode Decomposition DMD method. As shown in Figure 2, successive snapshots of the flow field variables with the same time interval Δt are preprocessed to form column vectors, and then the column vectors of each time snapshot are combined to form a matrix V_1^N.

$$V_1^N = \{v_1, v_2, v_3, \cdots, v_N\} \quad (1)$$

Among them, v_i represents the i-th flow field variable snapshot, and N is the number of selected flow field variable snapshots. Our goal is to build a linear dynamic system A. Among them, $\frac{d\vec{v}}{dt} = A\vec{v}$. Linear system A transforms present data v_{i-1} into future data v_i. Therefore, the linear dynamic system A satisfies the following conditions.

$$V_2^N = AV_1^{N-1} \quad (2)$$

Where V_2^N represents the future moment of V_1^{N-1}. A linear dynamical system can be represented

using the pseudo-inverse matrix $(V_1^{N-1})^{\dagger}$ of V_1^{N-1}.

$$A = V_2^N (V_1^{N-1})^{\dagger} \tag{3}$$

Linear dynamic system Least squares fit the present state and future state, and we call this exact DMD.

As shown in Equation 4, perform singular value (SVD) decomposition on the data at the present moment.

$$V_1^{N-1} = U \Sigma Y^* \tag{4}$$

Generally speaking, due to the high dimensionality of V_1^{N-1}, this results in excessive computation. So we use the low-rank structure for SVD. It can be represented as follows:

$$V_1^{N-1} = U_r \Sigma_r Y_r^* \tag{5}$$

So the linear dynamic system $A_{n\times n}$ can be expressed as Equation 6 by replacing the pseudo-inverse of V_1^{N-1}

$$A_{n\times n} = V_2^N (V_1^{N-1})^{\dagger} = V_2^N Y_r \Sigma_r^{-1} U_r^* \tag{6}$$

Although the linear dynamic system $A_{n\times n}$ has been calculated, its dimension is still too large, and the following transformation is applied to reduce its dimension:

$$\begin{aligned} A_{r\times r} &= U_r^* A U_r = U_r^* (V_2^N Y_r \Sigma_r^{-1} U_r^*) U_r \\ &= U_r^* V_2^N Y_r \Sigma_r^{-1} \end{aligned} \tag{7}$$

Now the low-dimensional linear dynamic system $\tilde{A}$ can be defined as:

$$\tilde{A} = A_{r\times r} \in \mathbb{R}^{r\times r}, r \ll n. \tag{8}$$

$\tilde{A}$ is a low-dimensional linear dynamic system, which is simple to calculate the eigenvalue and eigenvector:

$$\tilde{A} W = W \Lambda \tag{9}$$

Where W is the eigenvectors and Λ is the eigen values

In the previous steps, the feature vector W is calculated in the low-dimensional space, and the W obtained by the low-dimensional calculation can be returned to the original high-dimensional space by the following algorithm.

$$\Phi = V_2^N {}_{ir} \Sigma_r^{-1} W \tag{10}$$

Among them, Φ is the dynamic modal decomposition mode (DMD modes) of the original space, and the eigenvalue Λ has not changed.

Through the obtained linear dynamic system, the eigenvector Φ and eigenvalue Λ are obtained by calculation, and then the variable v is calculated using the eigenvector and eigenvalue to achieve the purpose of reconstructing and predicting the flow field by using the decomposition mode.

$$v(t) = \Phi e^{\Omega t} b = \sum_{k=1}^{r} \phi_k e^{wkt} b_k \tag{11}$$

3 DYNAMIC MODE DECOMPOSITION(DMD)

As shown in Figure 3, the middle three cavitation periods were selected for analysis, with times of 0.1938s-0.8750s and a cavitation frequency of 4.404Hz. The DMD decomposition is performed using velocity sequences in the flow field with a sampling interval of 0.0025s. Each cavitation cycle contains 90 snapshots of the flow field, for a total of 270 snapshots.

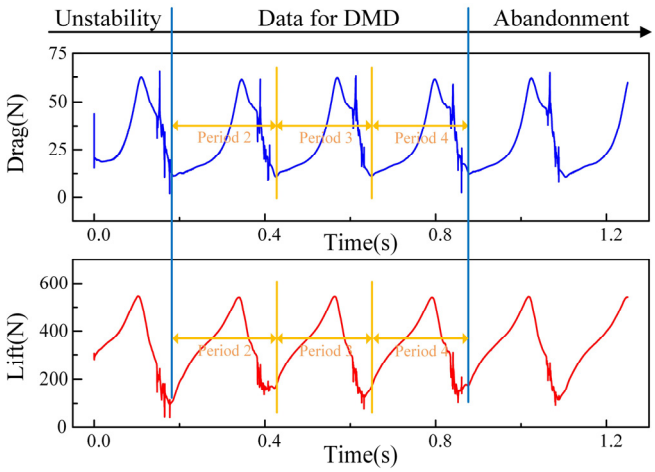

Figure 3: The periodicity of cavitation.

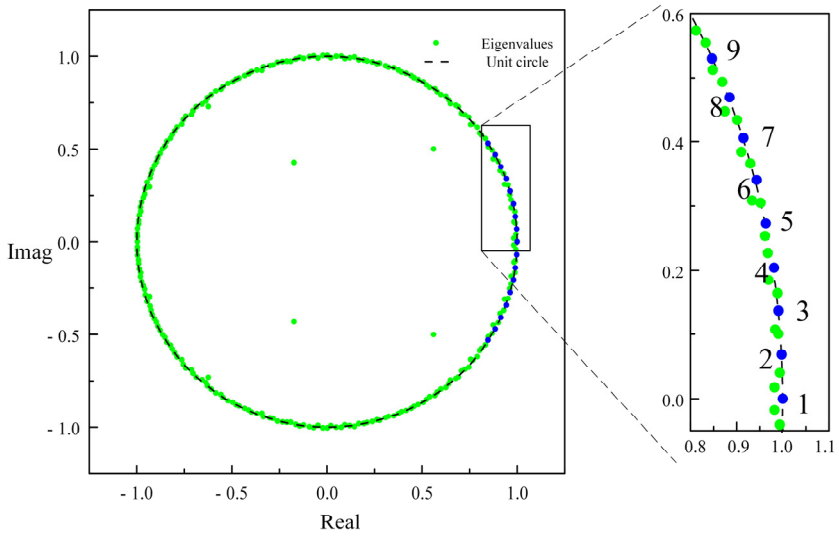

Figure 4: Eigenvalues in the complex plane.

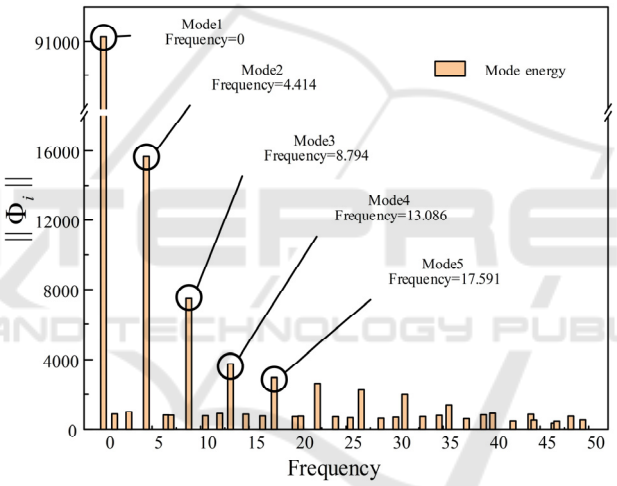

Figure 5: Dynamic mode energy at different frequencies.

Figure 4 shows the distribution of eigenvalues corresponding to different modes in the complex plane, with the horizontal coordinates representing the real part and the vertical coordinates representing the imaginary part. It can be seen that the eigenvalue distribution is symmetric along the real axis of the complex plane, indicating that the eigenvalues appear conjugately. The black dashed line represents the unit circle, and the relative positions between the eigenvalue points and the unit circle reveal the respective properties of the corresponding modes. The eigenvalues inside the unit circle indicate that this mode is convergent, and the modes outside the circle gradually increase in instability and eventually are divergent. Concurrently, the modes located on the unit circle are stable and do not change with time. Almost all eigenvalues are within the unit circle indicating good convergence of each mode after mode decomposition. The modes on the unit circle represent the linear characteristics of the cavitation process, while the rest represent the nonlinear characteristics. The cavitation process explored in this study has evident periodicity. Most of the modes are located near the unit circle, which verifies the stability and simulation accuracy of the cavitation period in this study.

Figure 5 shows the energy and frequency of each mode obtained by DMD, where the 2-norm of the modes defines the energy. According to the energy of each mode, Mode1 is the most energetic mode with a frequency of 0Hz, which represents the average flow field characteristics. The energy of Mode2 decreases

significantly, but the energy of Mode2 is still more considerable than other modes, and its frequency is 4.414 Hz, which is consistent with the cavitation frequency. Mode3-5 energy gradually decreases, while the frequency of the modes gradually increases, and the frequencies are multiples of the cavitation frequency.

4 RESULT AND DISCUSSION

Figure 6 shows the modes obtained after DMD of the axial velocity flow field data, and the longitudinal section of the flow field is intercepted for display. Where Re(phix) is the real part of the selected mode, the magnitude of its absolute value represents the magnitude of the regional energy, and positive or negative represents the change of phase. Mode1 is the average mode of the flow field, representing the flow field's primary flow structure and plays a dominant role in the whole cavitation process. The frequency of Mode2 is consistent with the cavitation frequency, which indicates that the critical periodically changing structure in the flow field is captured. It can be seen that the high-energy region of Mode2 is the same as the cavitation region, indicating that Mode2 responds to the cavitation region during the flow process. It can be seen that the distribution of the high-energy regions of Mode3 and Mode4 alternate along the velocity direction, and the frequencies of these two Modes are multiples of the cavitation frequency, representing the stretching off in the cavitation process. Mode6 and Mode8 have higher frequencies and lower energies. The contour shows that the energy of the high-energy region alternates along the hydrofoil suction surface and the direction of cavitation development. The energy of the high-energy region also decreases gradually along the flow direction. It represents the alternating shedding of cavitation and the high-frequency characteristics in some flow fields.

Figure 7 shows the 3D vortex structure(Q-criteria=1000) of different Modes in the flow field. The cavitation process of the hydrofoil is distributed in three dimensions in the flow channel, which is a typical flow with three-dimensional spatial characteristics. Because the middle of the hydrofoil is unaffected by shear forces on both sides of the wall, cavitation is more intense. The selected longitudinal section of the flow field can only show part of the characteristics of the cavitation process. To explore the flow field characteristics in more detail, need to analyze the three-dimensional characteristics.

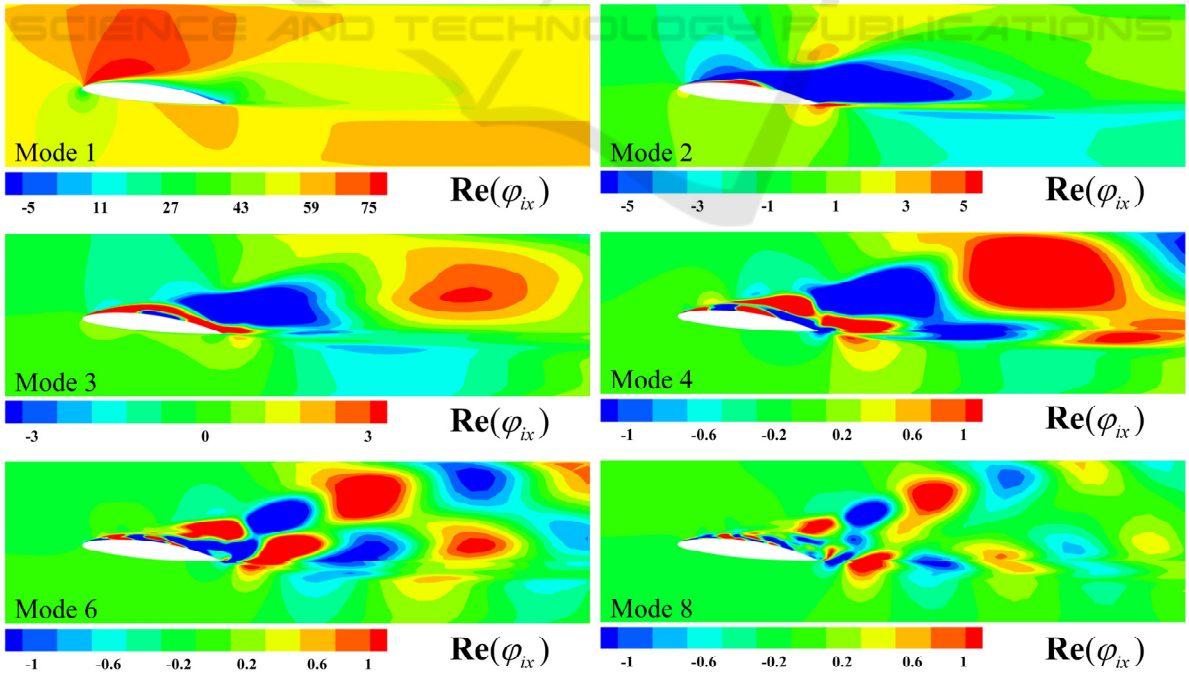

Figure 6: Different Modes in longitudinal plane of the flow field.

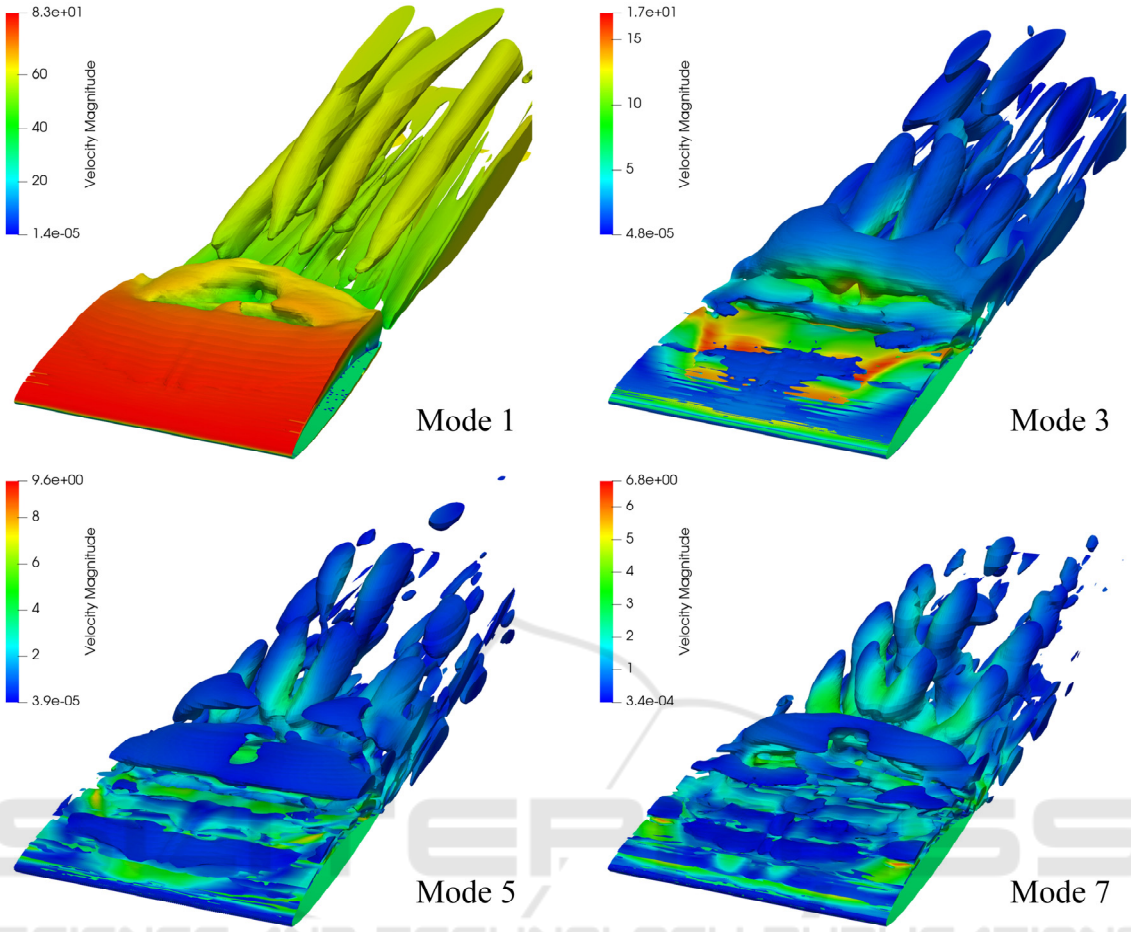

Figure 7: 3D vortex structure(Q-criteria=1000) of different Modes in the flow field.

5 CONCLUSION

In this study, the unsteady cavitation process of NACA66 was analyzed using DMD. It is found that the eigenvalues corresponding to different modes are symmetrically distributed along the real axis on the complex plane, indicating that the eigenvalues are conjugated. The eigenvalues are almost above the unit circle, indicating that the modes obtained by decomposition are convergent and have stable linear characteristics, while the modes corresponding to the eigenvalues deviating from the unit circle have nonlinear characteristics. The cavitation studied in this study has obvious periodicity. Most of the modal eigenvalues are located on the side of the unit circle, which verifies the accuracy of the simulation and DMD decomposition. At the same time, the cloud images of different modes are displayed, and the frequency energy of different modes is analyzed. These different modes capture the flow characteristics at different frequencies. The average mode represents the main flow structure of the flow field and plays a dominant role in the entire flow process. Mode2 represents the cavitation region, Mode3 and Mode4 represent the pull-off of cavitation, and higher-order modes represent the alternate shedding of cavitation and some high-frequency characteristics in the flow field. The research in this study is of great significance for us to understand the three-dimensional characteristics of the flow field and the three-dimensional dynamic modal characteristics in the cavitation process.

ACKNOWLEDGEMENT

The authors gratefully acknowledge the support of the National Natural Science Foundation of China (no. 51675315).

REFERENCES

Asnaghi A, Svennberg U, Bensow RE, et al. Numerical and experimental analysis of cavitation inception behaviour for high-skewed low-noise propellers. *Applied Ocean Research*. 2018, 79:197-214.

Dang Z, Mao Z, Tian W. Reduction of hydrodynamic noise of 3d hydrofoil with spanwise microgrooved surfaces inspired by sharkskin. *Journal of Marine Science and Engineering*, 2019, 7(5): 136.

Taira K, Hemati MS, Brunton SL, Sun Y, Duraisamy K, Bagheri S, Dawson ST, Yeh CA, et al. Modal analysis of fluid flows: *Applications and outlook. AIAA journal*. 2020, 58(3):998-1022.

Taira K, Brunton SL, Dawson ST, Rowley CW, Colonius T, McKeon BJ, Schmidt OT, Gordeyev S, Theofilis V, Ukeiley LS, et al. Modal analysis of fluid flows: An overview. *AIAA Journal*. 2017, 55(12):4013-41.

Liu M, Tan L, Cao S,et al. Dynamic mode decomposition of cavitating flow around ALE 15 hydrofoil. *Renewable Energy*. 2019, 139:214-27.

Chen KK, Tu JH, Rowley CW, et al. Variants of dynamic mode decomposition: boundary condition, Koopman, and Fourier analyses. *Journal of nonlinear science*. 2012, 22(6):887-915.

Jovanović MR, Schmid PJ, Nichols JW, et al. Sparsity-promoting dynamic mode decomposition. *Physics of Fluids*. 2014, 26(2):024103.

Kou J, Zhang W, et al. An improved criterion to select dominant modes from dynamic mode decomposition. *European Journal of Mechanics-B/Fluids*. 2017, 62:109-29.

Grilli M, Schmid PJ, Hickel S, Adams NA, et al. Analysis of unsteady behaviour in shockwave turbulent boundary layer interaction. *Journal of Fluid Mechanics*. 2012, 700:16-28.